Electric quadrupole interactions at ^{181}Ta nuclei in monocrystalline β-Ga_2O_3

1997 J. Phys.: Condens. Matter 9 6313

(http://iopscience.iop.org/0953-8984/9/29/016)

J. Phys.: Condens. Matter **9** (1997) 6313–6322. Printed in the UK PII: S0953-8984(97)79898-9

Electric quadrupole interactions at ^{181}Ta nuclei in monocrystalline β-Ga_2O_3

J Shitu and A F Pasquevich

Departamento de Física, Universidad Nacional de La Plata, c.c. No 67, 1900 La Plata, Argentina

Received 28 November 1996, in final form 17 April 1997

Abstract. A single crystal of β-Ga_2O_3 has been doped with ^{181}Hf by ion implantation. The time differential perturbed-angular-correlation technique has been applied to obtain information on the electric field gradients at the ^{181}Ta impurity. This impurity results from the β-decay of the implanted ions. Measurements were carried out at different temperatures and crystal orientations. The directions of the principal axes of the electric field gradient in relation to the crystal axes were deduced. The results are compared with those of similar experiments using ^{111}In as the implanted impurity in the same material, and with the quadrupole interactions of ^{181}Ta in HfO_2.

1. Introduction

The perturbed-angular-correlation (PAC) method is a powerful tool for the determination of electric field gradients (EFG) at atomic sites in solids. PAC measurements require a radioactive probe with appropriate nuclear properties at the site where the EFG will be measured. In the last ten years the technique has been intensively applied to EFG determinations at impurity sites in oxides. Most of the data have been obtained using ^{111}Cd as a probe [1]. More recently the interest has increased in getting experimental information on the EFG experienced by the other useful probe, ^{181}Ta, in the same hosts. The aim is to try to correlate both sets of results, in order to establish the role of the impurity as regards the measured EFG [2]. Depending on crystalline parameters, different behaviours can be observed. In the case of some oxides with bixbyite structure, where there are two non-equivalent sites for substitution of metal ions, the values measured for the quadrupole interaction frequency at the two sites using ^{181}Ta and ^{111}Cd are proportional [2]. The constant ratio, related to the Sternheimer factors and quadrupole moments of the two probes, shows that both probes act like 'observers', without distorting the atomic array in their surroundings. On the other hand, for bixbyite oxides with smaller lattice parameters and smaller metal–oxygen distances, such as In_2O_3, the PAC results indicate that Hf, or its daughter Ta, distorts the lattice [3].

In the present paper, we extend such comparisons to the case of single-crystalline β-gallium oxide. This oxide offers both fourfold- and sixfold-oxygen-coordinated cation sites. The oxide has already been characterized by PAC using the $^{111}\text{In} \rightarrow {}^{111}\text{Cd}$ probe. In these experiments, the ^{111}In activity was introduced by both chemical doping [4] and by In implantation [5]. In both cases, only one cation site was preferentially populated by indium: the sixfold-coordinated one.

In this paper, PAC results obtained after ^{181}Hf implantation in a β-Ga_2O_3 single crystal are described. The use of single crystals allows us to determine the orientation of the

0953-8984/97/296313+10$19.50

principal axes of the EFG tensor at the probe site. This knowledge makes it possible to go further in the comparison between the EFG experienced by both probes. Additional motivation for the investigation was provided by the desire to determine whether some features appearing in the experiments using the impurities ^{111}In and ^{111}Cd were also present in the cases where ^{181}Hf and ^{181}Ta were used. These features are as follows.

(i) Below a critical temperature T_C, a broadly distributed quadrupole interaction appears. This fact is attributed to the localization of an electronic defect (hole) in the neighbourhood of the acceptor impurity ^{111}Cd. In order to establish a more solid basis for such a conclusion, the PAC response when using a donor impurity as a probe seems to be important.

(ii) As a related topic, the question of charge compensation arises. The compensation can occur as a result of the appearance of a lattice defect or as a result of a change in the state of charge of the ions in the neighbourhood of the impurity.

(iii) It is of interest to find out whether hafnium has the same preference for the sixfold-coordinated site in the oxide structure as indium. If such a preference is essentially for size reasons, a similar behaviour can be expected from hafnium, since the ionic radius of hafnium is about the same as that of indium.

In addition, we carried out a few PAC measurements on ^{181}Hf:HfO_2 as a function of sample temperature in order to detect the possible formation of hafnium oxide precipitates in the case of Hf implantation in gallium oxide.

Results of PAC measurements on β-Ga_2O_3 using the probe $^{111}\text{In} \rightarrow {}^{111}\text{Cd}$ relevant for comparing with those of the present experiment are given in the next section.

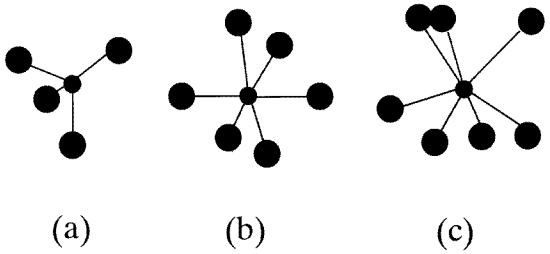

Figure 1. Gallium coordination polyhedra at both sites in β-Ga_2O_3: (a) tetrahedral; (b) octahedral. (c) The Hf coordination polyhedron in monoclinic HfO_2 is also shown.

2. Structure and properties of β-Ga_2O_3

β-Ga_2O_3 is the most stable gallium oxide phase. The crystallographic structure [8] is monoclinic. The lattice parameters are $a = 12.23$ Å, $b = 3.04$ Å, $c = 5.80$ Å, $\alpha = \gamma = 90^\circ$, and $\beta = 103.7^\circ$. The structure consists of a distorted cubic close-packed array of oxygen ions. There are two crystallographically non-equivalent gallium sites in the unit cell. Each Ga_I^{3+} is surrounded by a distorted tetrahedron of oxygen ions. The average Ga–O distance is 1.83 Å. Each Ga_{II}^{3+} is surrounded by a distorted octahedron of oxygen ions, the average distance being 2.00 Å. Both configurations of ions are shown in figure 1. The oxygen coordination of Hf in monoclinic HfO_2 is also shown, and it will be used in the discussion. We take the average distance Hf–O in this oxide (2.15 Å) as an indication of the space required for Hf, in order to choose either one or the other site in the structure. The lattice parameters of monoclinic HfO_2 are: $a = 5.15$ Å, $b = 5.20$ Å, $c = 5.32$ Å, and $\beta = 99.19^\circ$ [9].

Optical, magnetic, and hyperfine properties of several impurities in β-Ga_2O_3 have been reported (see the references quoted in reference [5]). Among all of the systems investigated,

the case of doping with Zr [10] is the most similar to the one reported here, taking into account the chemical similarity between Zr and Hf. In that case, an increase of the ionic conductivity with doping was observed, and it was attributed to the formation of gallium vacancies. This observation is important to the discussion of the compensation mechanism occurring in gallium oxide doped with hafnium.

In PAC studies of $^{111}\text{In} \rightarrow {}^{111}\text{Cd}$ as a probe in β-Ga_2O_3, where ^{111}In was introduced both chemically [4] and by implantation [5], it was found that the impurity replaces Ga preferentially at one of the possible sites in the monoclinic structure: the Ga_{II} site. For measurement temperatures lower than 585 K a strong damping occurs. At high temperatures there exists a well defined quadrupole interaction which is assigned to the ionized impurity centre. This interaction involves all of the probes in chemically doped samples, and around 70% in the case of samples prepared by implantation. The quadrupole interaction parameters are

$$\nu_Q = 119.1_1 \text{ MHz} \qquad \eta = 0.13_1 \qquad \delta < 0.01_1.$$

The results concerning the EFG axis orientation indicate that the direction of the principal axis z is normal to the monoclinic plane a–b, a direction which we denote with the vector $\boldsymbol{e}_3$. We will give the coefficients S_{2n} associated with this quadrupole interaction, together with the coefficients determined in the present paper.

3. Experimental details

The single crystal was grown under flux, and was kindly supplied by Professor Gunsser. ^{181}Hf ions were implanted at the Institut für Strahlen- und Kernphysik der Universität Bonn (Germany). The implantation energy was 160 keV, and the dose was 10^{13} ions cm^{-2}. The mean range of the implanted ions was 310 Å. The implantation was carried out along the monoclinic b-axis. For the measurements in hafnium oxide, a high-purity powder sample was irradiated with thermal neutrons to produce ^{181}Hf.

The PAC measurements were carried out on the 133–482 keV γ–γ cascade of ^{181}Ta. The PAC spectra were taken with a set-up of four BaF_2 detectors arranged in a 90° geometry. $R(t)$ perturbation functions were determined from the eight simultaneously measured PAC spectra, as is usually done for polycrystalline samples. The $R(t)$ data were Fourier transformed as described elsewhere [11]. Theoretical perturbation factors of the form $A_{22}G_2(t)$ folded with the measured time resolutions were fitted to the experimental $R(t)$ ratio. The time resolution associated with each of the eight spectra, obtained as the full width at half-maximum of the measured 'prompt' curves, were in the range 0.7–0.9 ns. For the fitting procedure, only one of these curves was used.

For a static quadrupole interaction, the perturbation factor has the form

$$G_2(t) = \sum_{n=0}^{3} S_{2n} \mathrm{e}^{-\delta\omega_n t} \cos(\omega_n t).$$

The frequencies ω_n are related to the quadrupole frequency $\nu_Q = eQV_{zz}/h$ by $\omega_n = g_n(\eta)\nu_Q$. The coefficients $g_n(\eta)$ are known functions of the asymmetry parameter $\eta = (V_{xx} - V_{yy})/V_{zz}$, where the V_{KK} $(K = x, y, z)$ denote the principal components of the EFG tensor. The exponential function accounts for a Lorentzian frequency distribution δ around ω_n. In the case of single crystals, the coefficients S_{2n} depend on both η and the angles between the emission direction of the γ-rays and the principal axes of the EFG tensor. Details of this dependence can be found elsewhere [6]. In order to specify the orientation of the single crystal during the measurements, we define a polar axis normal to the detector

plane, and an azimuthal axis along one of the lines joining opposite detectors. The spectra at different orientations will be labelled with the angles θ_2, ϕ_2, θ_3, ϕ_3 that two crystalline vectors $\boldsymbol{e}_2$, $\boldsymbol{e}_3$ make with such axes. If $\theta = 0^\circ$, then ϕ has no meaning, and we will put $\phi = u$ (undefined). We define the orthonormal set of vectors ($\boldsymbol{e}_1$, $\boldsymbol{e}_2$, $\boldsymbol{e}_3$) as follows: $\boldsymbol{e}_1$ and $\boldsymbol{e}_2$ lie along the monoclinic axes b and a respectively, and $\boldsymbol{e}_3 = \boldsymbol{e}_1 \times \boldsymbol{e}_2$. The principal axes of the EFG tensor are called x, y, and z. The errors in the angles specifying the crystal orientations were estimated to be less than 5°.

4. Results

As expected, the PAC spectrum after implantation corresponds to a broad distribution of quadrupole frequencies due to the damage produced by the implantation. The first step in our investigation was that of studying the annealing of the radiation damage. Annealings in the open air were carried out, followed by PAC measurements at room temperature. Both the temperature and the sequence of the annealing treatments were the same as those used in the experiment performed following In implantation described in reference [5].

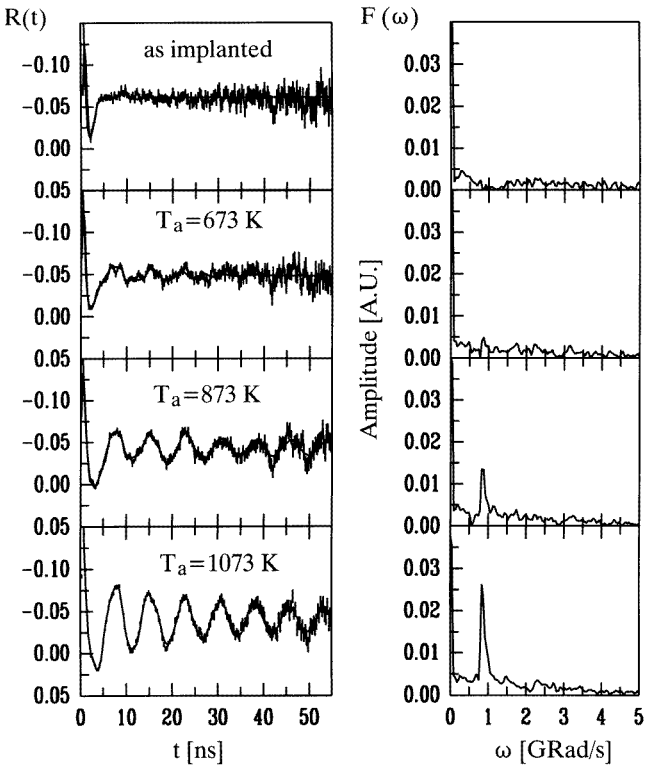

Figure 2. PAC results obtained after annealing at the temperatures indicated. $R(t)$ spectra and their Fourier transforms are shown.

In figure 2, PAC results obtained after annealing for 30 minutes at the temperatures indicated are shown. The orientation of the crystal during these measurements was such that the monoclinic axes a and b were in the plane of the detectors, forming angles of 45° with the lines joining opposite detectors, i.e. $(90^\circ, 45^\circ, 0^\circ, u)$. After the treatment at the highest temperature, the spectrum can be fitted assuming the existence of two fractions of atoms in the crystal: one fraction f_1 undergoing a well defined quadrupole interaction, and the other, f_2, undergoing a broadly distributed interaction. The minor fraction f_1 is

responsible for the periodic pattern in the spectrum, giving the peak in the Fourier transform. The coefficients S_{2n} for this component were obtained by the fitting procedure, and they will be given below. The fraction f_1 is around 30%, and the parameters characterizing the quadrupole interaction at room temperature are

$$\nu_{Q1} = 753(13)\ \text{MHz} \qquad \eta_1 = 0.40(1) \qquad \delta_1 = 0.02(1).$$

Actually, these values are in each case averages of a couple of measurements at room temperature.

The S_{2n}-coefficients for the component f_2 were taken as corresponding to a poly-crystalline material, due to the broad frequency distribution. The parameters associated with this fraction at room temperature are

$$\nu_{Q2} = 834(32)\ \text{MHz} \qquad \eta_2 = 0 \qquad \delta_2 = 0.56(6).$$

The contribution of this fraction of probes to the spectrum is damped in a short time, and gives rise to the 'hard-core' value which appears as a base-line in the spectrum.

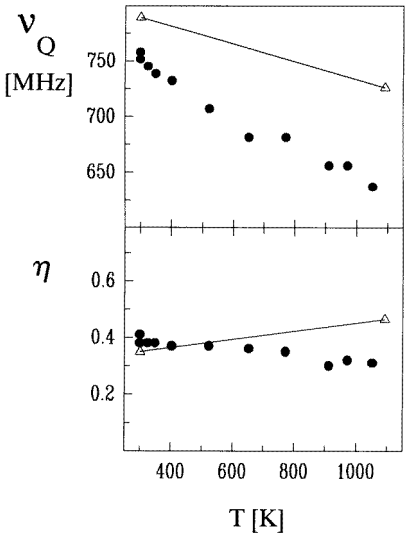

Figure 3. Hyperfine parameters corresponding to fraction f_1 of probes in β-Ga_2O_3 as a function of the temperature. The lines show the temperature dependence expected for the frequency and for the asymmetry parameter for the case of HfO_2.

PAC spectra were taken at temperatures between room temperature and 1043 K. The parameters corresponding to the well defined quadrupole interaction are shown in figure 3 as functions of the temperature. The f_2-component remains a broadly distributed quadrupole interaction over the complete temperature range.

We have also carried out PAC measurements on HfO_2 at several temperatures, in order to detect precipitates of this oxide. Our results at room temperature are

$$\nu_Q = 787(4)\ \text{MHz} \qquad \text{and} \qquad \eta = 0.38(1)$$

in good agreement with the data reported in the literature [7]. The lines in figure 3 show the temperature dependences measured for ν_Q and η for HfO_2.

Spectra taken at different crystal orientations and obtained at 1050 K are shown in figure 4. The orientations of the crystallographical axes $\boldsymbol{e}_2$ and $\boldsymbol{e}_3$, with respect to the detectors (black squares), are shown in the circles, and specified by the angles given in the figures. The fitted values of the S_{2n}-parameters corresponding to each orientation are given in table 1. The amplitudes of the Fourier peaks in figure 4 are related to these coefficients. But, additionally, the amplitudes are affected both by the frequency distribution δ and by

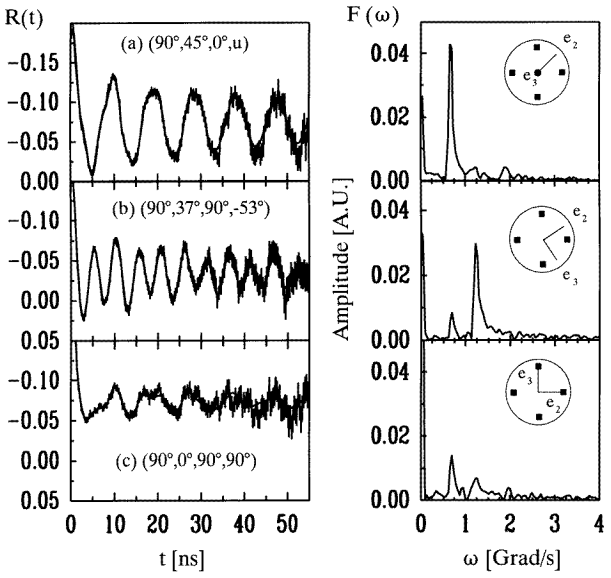

Figure 4. PAC spectra taken at different crystal orientations. The crystal orientation is defined by the positions of the vectors $\boldsymbol{e}_2$ and $\boldsymbol{e}_3$ relative to the detectors. This position is in each of (a), (b), and (c) given by the angles on the left and schematically drawn in the circles on the right, where the detectors are represented by squares.

Table 1. Measured S_{2n}-parameters for different crystal orientations. The errors were estimated to be $\sim$0.04.

Orientations	S_{20}	S_{21}	S_{22}	S_{23}
(90°, 45°, 0°, *u*)	0.00	0.83	0.06	0.11
(90°, 37°, 90°, −53°)	0.07	0.16	0.77	0.00
(90°, 0°, 90°, 90°)	0.70	0.17	0.10	0.03

the finite time resolution. For the typical measured values of $\nu_Q = 635$ MHz, $\eta = 0.31$, and $\delta = 0.02$, the frequency distribution produces additional reductions of 23, 38, and 47% in the amplitude associated with ω_1, ω_2, and ω_3 respectively. The finite time resolution produces additional reductions of 12, 15, and 23% in the peak amplitudes.

5. Discussion

In connection with the removal of the radiation damage on annealing, it is interesting to compare the present results with those obtained in the experiments performed after ^{111}In implantation described in reference [5]. Although the implantation energy was higher (400 keV) and the duration of the annealing treatments was longer (120 min) than those in the present case (160 keV, 30 min), the PAC results at each annealing stage are quite similar. This is not surprising, because 30 minutes is a long enough annealing time to allow the recovery that the annealing temperature activates to be completed. The same annealing temperatures were used in the two experiments. As seen using both probes, the changes in the probe neighbourhood with the annealing treatments look the same, and this is an

indication that only lattice recovery is involved in such modification. After the annealing at the highest temperature, a fraction f_1 of probes is located in a regular lattice site without defects or distortions in its neighbourhood. Furthermore, the measured values of the S_{2n} behave as expected for the single crystal; only one peak appears in the Fourier transform. We conclude that this site is one of the cationic sites in the oxide. The nature of the other fraction is very uncertain; it can include probe atoms near the surface, atoms in Hf-vacancy clusters, and probes in small amorphous regions.

Therefore, we will restrict the discussion to the well defined interaction. Because of the similarity between the parameters characterizing this interaction at room temperature and the ones corresponding to those observed for HfO_2, we considered the possibility of the formation of oxide precipitates during the annealing. Although in previous experiments based on Hf implantation in oxides such precipitation has never been observed, the present case could be more favourable, taking into account the large difference between the ionic radii of Ga^{3+} and Hf^{4+}. However, the fact that the behaviour on annealing seems to be the same when monitored with either probe, as mentioned above, excludes the possibility of the formation of precipitates. Another feature found in the quadrupole interactions of ^{181}Ta in the monoclinic phase of hafnium oxide (which is the stable one in the temperature range of the measurements) is the increase of η with temperature. This behaviour is certainly opposite to that observed for β-Ga_2O_3. Therefore we can take the interaction I_1 as characteristic of Hf diluted in the β-Ga_2O_3 phase. The existence of only one well defined interaction in a crystal where there are two sites for substitution is related to preferential occupation. This characteristic of the impurity substitution in gallium oxide has been observed before, as was already mentioned in the introduction. In the experiments using a $^{111}In \rightarrow {}^{111}Cd$ probe, it has been found that indium substitutes for gallium only at the site Ga_{II}, and, taking into account the fact that In^{3+} and Hf^{4+} have the same radius, 0.81 Å, it is reasonable to assume that they occupy the same kind of site in the structure.

Additional arguments are as follows. We can compare the distances Ga–O at both sites with the distance Hf–O in compounds where Hf is either a normal constituent or an impurity. The average Ga–O distances are 2.00 Å and 1.83 Å for the octahedral and tetrahedral sites, respectively. Hf seems to require a longer metal–oxygen distance. Such a distance is greater than 2.16 Å in the oxides with bixbyite structure, where hafnium as an impurity does not introduce distortions [2]. In the monoclinic phase of HfO_2, which is the stable one at room temperature, the distance is 2.15 Å. This length could be taken as an indication of the space required by hafnium. However, lower Hf–O distances have been observed, for example, in Hf:$NbLiO_3$ [12], where such distance is 2.07 Å. Then, in gallium oxide, the octahedral site appears to be more favourable for hafnium occupation, because there is more room in it.

On the other hand, we can take into account the four- and six-oxygen coordination existing at both sites in gallium oxide. In all of the compounds mentioned above, the hafnium is coordinated with six or more oxygens (the exception is the monoclinic phase of HfO_2, where the coordination is seven). Then, in beta gallium oxide, the sixfold-coordinated site is more favourable.

It is worth mentioning that the simple size considerations invoked above can lead to incorrect site assignments, as has been established for some ternary oxides [13], but they probably work well in the present case, where only one kind of metallic ion is available for substitution. We would like now to compare the hyperfine parameters obtained in the present experiment with those obtained using the $^{111}In \rightarrow {}^{111}Cd$ probe. When EFG measurements using different probes are compared, the measured η-values provide a first account of the distortions produced by the probes. The η-values measured with the $^{181}Hf \rightarrow {}^{181}Ta$ probe lie in the range $\eta = 0.42$–0.32, and for the case with the $^{111}In \rightarrow {}^{111}Cd$ probe they lie in

the range $\eta = 0.11$–0.20. The differences are probably due to the quite different electronic structures of the probes, which leads to different local contributions to the EFG. Adams and Catchen [14] have found even greater discrepancies in the cases of both probes in TiO_2. The point-charge model calculations applied, adding contributions of ions inside a sphere of radius 100 Å, give $\eta = 0.53$. The discrepancy between this and the measured values indicates non-ionic contributions to the EFG existing at both probe sites. When the measured value is reproduced by PCM calculations, it can be argued that the probe undergoes very little directional bonding [14].

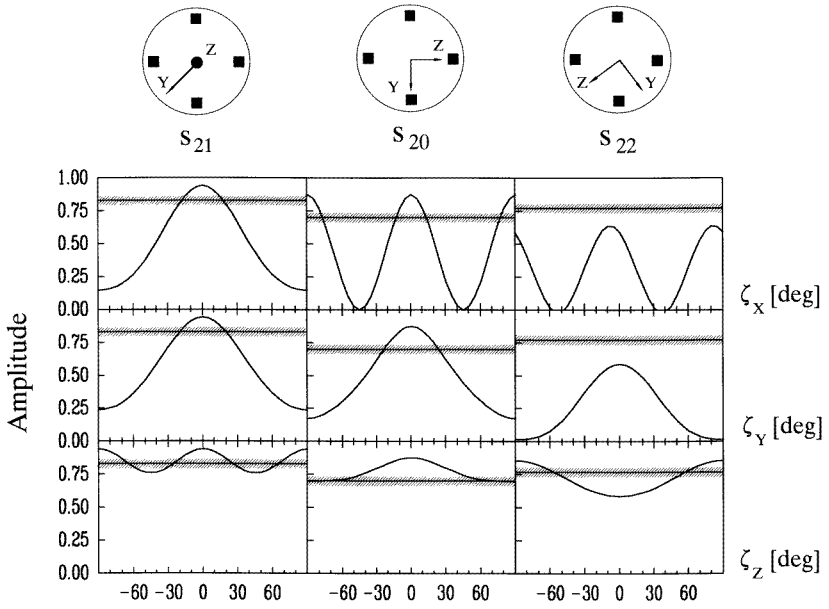

Figure 5. S_{2n}-values as functions of the orientation of the EFG axes relative to the detectors. In the circles, the EFG axes and the detectors (squares) are shown. In the boxes below the circles, the S_{2n}-coefficient which is the dominant one for each orientation is drawn. The values of such coefficients for the axis orientations drawn in the circles correspond to $\xi_i = 0°$. In each case, the expected variation of the coefficient with deviations of the EFG axes from the positions drawn in the circles is displayed as a function of the rotation angles around the initial axes. ξ_i denotes the rotation angle around the axis i $(i = x, y, z)$. The measured value for such a coefficient is shown as a band. The band width indicates the estimated error.

Let us discuss now the results on the EFG orientation. Figure 5 shows the values of the S_{2n}-coefficients calculated for different orientations of the x-, y-, and z-axes relative to the detector positions. The values were calculated for $\eta = 0.32$, and they are displayed as functions of the rotation angle ξ_i around the i-axis $(i = x, y, z)$, starting at the position shown in the inset ($\xi_i = 0$). In order to begin the discussion, we would like to point out that the experimentally determined S_{2n}-values indicate that the z-axis is roughly pointing in the direction of the e_3-axis. This can be inferred from the highest values of S_{2n} measured for the different crystal orientations (table 1): one expects a dominant S_{21}-value for z normal to the plane of the detectors, a dominant S_{22}-value for z lying between the detectors, and a dominant S_{20}-value for z aligned with two of the detectors. These results are qualitatively fairly similar to the ones found with ^{111}In for the principal interaction in β-Ga_2O_3. The directions for the axes x, y, and z, calculated using the point-charge model (PCM) (with

$R_c > 10$, R_c being the radius of the sphere, including the ions used in the calculation), give an xyz-set coincident with ($\boldsymbol{e}_1, \boldsymbol{e}_2, \boldsymbol{e}_3$). However, the comparison of the measured S_{2n}-values and the calculated ones displayed in figure 5 shows that the deviations of such directions agree better with the experimental results: the orientation $(90^\circ, 45^\circ, 0^\circ, u)$ suggests either a position of the z-axis forming an angle of 20° with $\boldsymbol{e}_3$ (rotation around x), or axes x, y rotated by approximately 60° around $\boldsymbol{e}_3$.

On the other hand, the value of S_{22} observed for the orientation $(90^\circ, 37^\circ, 90^\circ, -53^\circ)$ is higher than the one which corresponds to z along $\boldsymbol{e}_3$, and rotations of the z-axis around x- or y-axes cannot explain this result. However, a rotation around z, $\xi_z = 60^\circ$, gives the measured values.

The misalignment of the crystallographic axes and the principal axes of the EFG tensor is corroborated by the low value of S_{20} for the orientation $(90^\circ, 0^\circ, 90^\circ, 0^\circ)$ as compared with the calculated values shown in figure 5 for $\xi_i = 0^\circ$. In this case, the measured values can be explained by assuming one or the other of the rotations pointed out in the first case.

The analysis indicates that the principal axes x and y lie at 60° with respect to the axes $\boldsymbol{e}_2$ and $\boldsymbol{e}_1$, this being the common aspect in the rotations invoked above. The possibility of a small angle between $\boldsymbol{z}$ and $\boldsymbol{e}_3$ cannot be excluded, taking into account the errors involved in the angles defining the crystal orientation and those resulting from the fitting procedure.

Table 2. The coefficients S_{2n} determined in reference [6] for the principal interaction component in the experiment using the probe ^{111}In at crystal orientations which are comparable to the ones used in the present experiment.

Orientations	S_{20}	S_{21}	S_{22}	S_{23}
$(90^\circ, 45^\circ, 0^\circ, u)$	0.00	0.86	0.01	0.13
$(90^\circ, 45^\circ, 90^\circ, -45^\circ)$	0.00	0.20	0.80	0.00
$(90^\circ, 0^\circ, 90^\circ, 90^\circ)$	0.71	0.22	0.05	0.02

In table 2, the coefficients obtained using the probe $^{111}\text{In} \rightarrow {}^{111}\text{Cd}$ in single-crystalline β-Ga_2O_3 are shown for crystal orientations which are comparable to the ones reported in the present experiment. An interesting feature of the experimental result is that the EFG directions at the $^{111}\text{In} \rightarrow {}^{111}\text{Cd}$ and $^{181}\text{Hf} \rightarrow {}^{181}\text{Ta}$ probe sites agree fairly well. As is quoted by Forker and Vianden [15], there are cases where different probes in the same host experience different EFG orientations. This is connected with the different electronic structures of the impurities. In the comparison made here, the difference in the electronic structure of the probes results in differences in the local distribution of charge, which give rise to a different symmetry parameter, but the principal axis z is the same, and x and y are pointing roughly in the same directions, as can be inferred by comparing the S_{2n}-coefficients obtained in the two experiments.

The orientation is not collinear with the axes $\boldsymbol{e}_1, \boldsymbol{e}_2$, and $\boldsymbol{e}_3$, and this is not surprising. Such a set was introduced arbitrarily, in order to describe the crystal orientation during the measurements. The monoclinic structure prevents one from using symmetry considerations to anticipate the EFG orientation. Point-charge calculations indicate the axes $\boldsymbol{e}_1, \boldsymbol{e}_2$, and $\boldsymbol{e}_3$ as the principal ones, and the discrepancy with the experimental results is only as regards the directions of the x- and y-axes. Again this is not surprising, taking into account the existence of local contributions to the EFG, which are revealed by the disagreement of the calculated asymmetry parameters and those measured with the different probes. Despite the existence of these local contributions, the fact that the EFG points in the same direction at both probe sites indicates that they are surrounded by similar charge distributions. The

charge compensation must occur through a uniform distribution of the probe's extra electrons in the neighbouring ions, without involving any lattice defects.

6. Conclusions

We have characterized the hyperfine interactions of Hf implanted in β-Ga_2O_3, and found that the hyperfine parameters at room temperature are similar to the ones found for HfO_2, but, because of both the single-crystalline characteristics of the interaction and the temperature dependence, we conclude that the observed interaction corresponds to hafnium substituted into a gallium site in the crystal. The preferential site occupation is confirmed by the existence of only one well defined quadrupole interaction.

The directions of the EFG principal axes were established. The principal z-axis is normal to the monoclinic plane a–b. This direction coincides with the one observed using the probe $^{111}In \rightarrow {}^{111}Cd$. The principal axes x and y lie at 60° with respect to the monoclinic axes a and b, respectively. The discrepancy between this last result and the prediction of PCM calculations is due to local contributions to the EFG. All of this is consistent with similar discrepancies for the asymmetry parameter. On the other hand, the results confirm that the damping observed in PAC spectra below $T_C = 580$ K when using ^{111}Cd as a probe are connected with such impurity, and not with a particular host transformation.

Acknowledgments

This work was partially supported by the Consejo Nacional de Investigaciones Científicas y Técnicas (CONICET) and the Comisión de Investigaciones Científicas de la Provincia de Buenos Aires (CICPBA), Argentina. We thank Dr K Freitag from the Institut für Strahlen- und Kernphysik der Universität Bonn (Germany) for the ion implantations, and Professor W Gunsser (University of Hamburg, Germany) for providing the gallium oxide single crystals used in this study. We are greatly indebted to Professor M Forker for helpful discussions and comments on this work.

References

[1] Wiarda D, Uhrmacher M, Bartos A and Lieb K P 1993 *J. Phys.: Condens. Matter* **5** 4111
[2] Pasquevich A F, Bibiloni A G, Freitag K, Massolo C P, Rentería M and Vercesi J 1994 *Phys. Rev.* B **49** 14 331
[3] Vercesi J A, Bibiloni A G, Massolo C P, Moreno M S, Pasquevich A F and Freitag K 1993 *Phys. Rev.* B **47** 490
[4] Pasquevich A F 1990 *Hyperfine Interact.* **60** 791
[5] Pasquevich A F, Uhrmacher M, Ziegler L and Lieb K P 1993 *Phys. Rev.* B **48** 10 052
[6] Wegner D 1985 *Hyperfine Interact.* **23** 179
[7] Lerf A and Butz T 1987 *Hyperfine Interact.* **36** 275
Ayala A, Alonso R and López García A R 1994 *Phys. Rev.* B **50** 3547
[8] Geller S 1960 *J. Chem. Phys.* **33** 676
[9] Hann R E, Suitch P R and Pentecost J L 1985 *J. Am. Ceram. Soc.* **68** C285
[10] Harwig T, Wubs G J and Dirksen G J 1976 *Solid State Commun.* **18** 1223
[11] Scian A N, Aglietti E F, Caracoche M C, Rivas P C, Pasquevich A F and López García A R 1994 *J. Am. Ceram. Soc.* **77** 1525
[12] Prieto C, Zaldo C, Fessler P, Dexpert H, Sanz-García J A and Diéguez E 1991 *Phys. Rev.* B **43** 2594
[13] Catchen G L and Spaar D M 1991 *Phys. Rev.* B **44** 12 137
[14] Adams J M and Catchen G L 1994 *Phys. Rev.* B **50** 1264
[15] Forker M and Vianden R 1983 *J. Magn. Reson.* **7** 275